Gamma-Ray Irradiation Effects on CMOS Image Sensors

in Deep Sub-Micron Technology

Padmakumar R. Rao[1], Xinyang Wang[1], Adri J. Mierop[2], and Albert J.P. Theuwissen[1,2] (IEEE Fellow)
[1]Electronic Instrumentation Laboratory, Delft University of Technology,
Delft, the Netherlands
[2]DALSA, Eindhoven, the Netherlands
email: p.ramachandrarao@tudelft.nl, Ph: +31152781602, Fax: +31152785755

INTRODUCTION

CMOS Active Pixel Sensors (APS) excel in domains that include low power operation and on-chip integration of analog and digital circuitry. Since these sensors are utilized for applications involving the detection of signals as low as a few electrons, radiation tolerance of such devices is of primary concern. All possible radiation effects are usually grouped into three basic types: transient effects (not dealt in this study), ionization damage and displacement damages [1], [2], [6]. Ionization damage has been considered to be the dominant mechanism when energetic photons (γ and X-rays) interact with solid-state matter. The major concerns due to this damage are charge build-up in the gate dielectric and radiation induced interface states. The introduction of discrete energy levels at the $Si\text{-}Si0_2$ interface leads to increased generation rates and thus higher surface leakage currents. Similarly, displacement of lattice atoms in the bulk leads to modified minority carrier lifetimes and increased bulk-generated leakage currents [2], [3], [4], [5].

EXPERIMENTAL

"Pinned" CMOS photodiodes (Fig. 1) utilize a p^+ pinning layer that shields the photodiode from surface effects that contribute to the leakage mechanism. The doping of the layers are chosen such that the photodiode is depleted completely. One of the most dominant dark current mechanisms in these structures are the defective sidewalls and the edges of shallow trench isolations (STIs) separating the photodiodes [9], [10]. To test the effects of radiation, test-structures with and without p-well protected STIs (Shallow Trench Isolation) were fabricated in Philips' 0.18-μm CMOS technology (Table. 1). The gap between the STI and the photodiode is represented by the parameter NTA. The structures were tested by irradiating them with γ-rays (1.17 MeV, 1.33 MeV); dose rate of 75.9 Gray/min.

Solving the continuity equation of a usual p^+/n photodiode derives an analytic model for the internal spectral response of pinned photodiodes. An equivalent diode reverse voltage V_d, is used to represent the depleted diode. The contribution from the p-type epitaxial region is included for the contribution from carriers collected through diffusion. This model is used to estimate the optical degradation of the sensors due to irradiation. Standard CMOS process parameters have been used for the simulation.

The dispersive transport phenomenon in the SiO_2 can be modeled on the concept of *small polaron hopping*, called as CTRW (continuous-time random walk). The transport process varies with the fourth power of the oxide thickness rendering modern deep sub-micron process ($t_{ox} \approx 4\ nm$) radiation hard to ionization damage in the gate regions. We provide results that suggest that the degradation of the STIs due to irradiation is an important factor influencing the sensor performance in advanced technological processes where very thin oxides and small geometries are employed. The histograms of the dark signal of the sensors (Fig. 2 - 5; all different horizontal scales) reveal that the radiation-induced degradation mechanism is sensitive to the nature and the location of the STI. The largest degradation is seen in structures that have unprotected STIs (Fig. 6). Further, structures that have the STI closer (NTA = 0.2 μm) to the photodiode is seen to degrade faster than the structures that have the STI further apart (NTA = 0.3 μm). Since the doping density of the p-well region is relatively higher than that of n-type region of the photodiode, the STI is isolated from the depletion region during integration for structures with p-well protection [11]. This explains the lower dark signal from these structures, and also the slower degradation of these structures to irradiation. The Arrhenius plot of the dark current (Fig. 7), shows that the radiation process introduces levels in the band-gap that tends the activation energy towards $E_g/2$, conforming to a generation-recombination mechanism. A plot of the activation energies of some 1000 pixels as a function of dark current (Fig. 8) reveals a field-enhancement phenomenon that results in pixels with lower activation energies to exhibit larger leakage currents [4], [5], [7]. We have characterized this effect in a separate study [8]. Fig. 9 shows the normalized spectral response (sensors output

(DNs)/calibrated sensor output (A)) of radiated as well as un-irradiated sensors and the fit based on the model. The equivalent reverse voltage V_d for the model was found to be 1.2 V resulting in a total depletion width of ~ 1.6 μm. A very good fit for all the curves is obtained by using an attenuation factor ξ_i (acting through the front layer optical stack) as well as the term for surface recombination velocity, *s*. The change in the parameters ξ_i and *s* extracted through the model indicates monotonic optical stack as well as interface degradation for the dose range considered. High energy rays such as γ-rays change the properties of the materials they penetrate and mainly interact through electronic excitation, electronic ionization and atomic displacements. As a result, color centers are introduced in the material [12]. A change in the absorption characteristics of top layer optical stack can explain the attenuation observed. From Fig. 9, a smoothening of the sharp peaks found in the un-irradiated devices can be seen on radiated devices which can also be explained by this hypothesis. The variation of the lifetime in the epi-layer does not have much effect in the present sensor, with a thickness of ~ 4 μm.

CONCLUSION

1. The results indicate that p-well protected STI structures are inevitable for radiation-hard designs. A larger value of NTA results in higher immunity to radiation damage, but should be optimized to avoid loss of sensitivity and pixel saturation levels. 2. Radiation induced leakage mechanism is sensitive to field-enhancement processes, so efforts should be directed to reduce this effect especially in deep sub-micron technologies. 3. The results highlight the need to further study the changes in top-layer material characteristics due to radiation process, to improve sensor quality for future high-quality image sensing in harsh environments.

ACKNOWLEDGEMENTS

This work is funded by the Dutch Technology Foundation (STW) DSC5869 and Philips/DALSA for test structures. The authors wish to thank Martijn Snoeij, TUDelft; Peter Swart, DIMES; and personnel of I.R.I, Delft, for their valuable insights and technical assistance during the project.

REFERENCES

[1] J. Bogaerts, B. Dierickx, G. Meynants, and D. Uwaerts, “Total Dose and Displacement Damage Effects in a Radiation-Hardened CMOS APS”, *IEEE Trans. Elec. Dev,* 50(1), pp. 84–90, January 2003.

[2] C. Claeys and E. Simon, “Radiation Effects in Advanced Semiconductor Materials and Devices”. *Springer Series in Material Science*, 2002.

[3] E. S. Eid et al., “Design and Characterization of Ionizing Radiation-Tolerant CMOS Image APS Image Sensors 30 MRad (Si) Total Dose”, *IEEE Trans. Nucl. Sci.*, 48(6), pp. 1796–1806, 2001.

[4] G. R. Hopkinson, “Radiation Effects in a CMOS Active Pixel Sensor”, *IEEE Trans. Nucl. Sci.*, 47(6), pp. 2480–2484, December 2000.

[5] J. Bogaerts, *“Radiation-Induced Degradation Effects in CMOS Active Pixel Sensors and Design of a Radiation Tolerant Image Sensor”*, PhD thesis, pp. 5–15, 37–95, Katholieke Univ. Leuven, April 2002.

[6] X. T. Meng, A. G. Kang, J. H. Li, H. Y. Zhang, S. J. Yu, and Z. You, “Effects of Electron and Gamma-ray Irradiation on CMOS Analog Image Sensors”, 43, pp. 1151–1155, *Microelectron. Reliab.* 2003.

[7] M. Cohen, J. P. David, “Radiation-Induced Dark Current in CMOS Active Pixel Sensors”, *IEEE Trans. Nucl. Sci*., 47(6), pp. 2485-2491, December 2000.

[8] X. Wang, P. R. Rao and A. J. P. Theuwissen, “Fixed-Pattern Noise Induced by Transmission Gate in Pinned 4T CMOS Image Sensor Pixels”, *Proc. ESSDERC.*, pp. 331–334, September 2006.

[9] C. R. Moon, J. Jung, D. W. Kwon, J. Yoo, D. H. Lee and K. Kim, “Application of Plasma-Doping (PLAD) Technique to Reduce Dark Current of CMOS Image Sensors”, *IEEE Elec. Dev. Lett*., Vol. 28, No. 2, pp. 114–116, February 2007.

[10] L. S. Riley, S. Hall and J. Schitz, “Evaluation of Surface Generation Velocity of Sidewall Oxide Interfaces Formed by Dry Etching for Shallow Trench Isolation”, *Sol. St. Elec*., Vol. 44, No. 11, pp. 2093–2095, November 2000.

[11] H. I. Kwon, I. M. Kang, B. G. Park, J. D. Lee and S. S. Park, “The Analysis of Dark Signals in the CMOS APS Imagers From the Characterization of Test Structures”, *IEEE Trans. Elec. Dev*., Vol. 51, No. 2, pp. 178–184, February 2004.

[12] K. Arshak , O. Korostynska, “Gamma Radiation–induced Changes in the Electrical and Optical Properties of Tellurium Dioxide Thin Films”, *IEEE Sensor Journal*, Vol. 3, No. 6, December 2003.

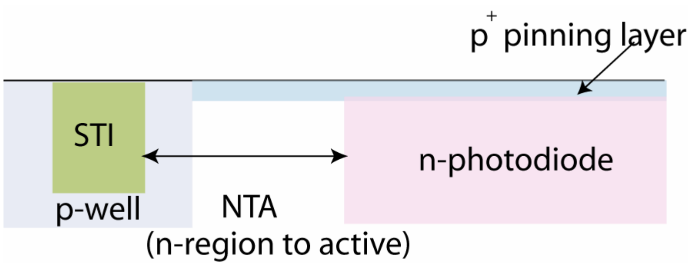

Figure 1: Layout schematic of the pixels.

Parameter	Value
Pixel pitch	3.5 µm
Conversion gain (g) (photon shot-noise method)	39.7 $\mu V/e^-$
Transfer gate length	0.6 µm
Operating voltage	3.3 V
Integration time	6.4 ms

Table 1: Sensor and measurement details.

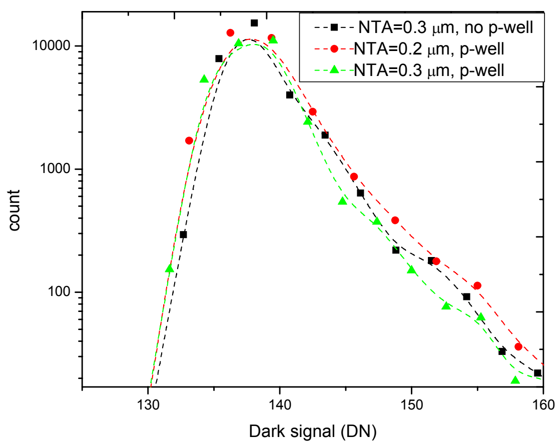

Figure 2: Histogram of the dark signal for the unradiated sensors.

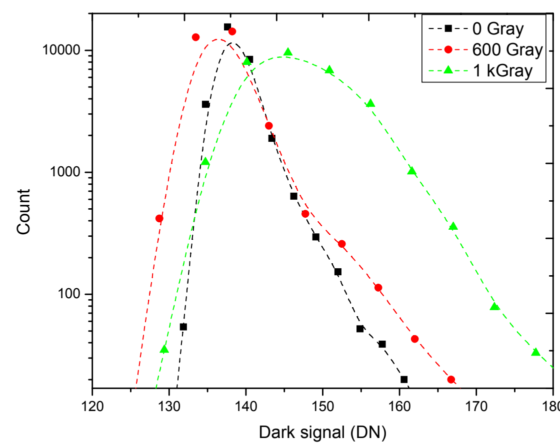

Figure 3: Histogram of the dark signal for sensor with NTA=0.3 µm, p-well protected.

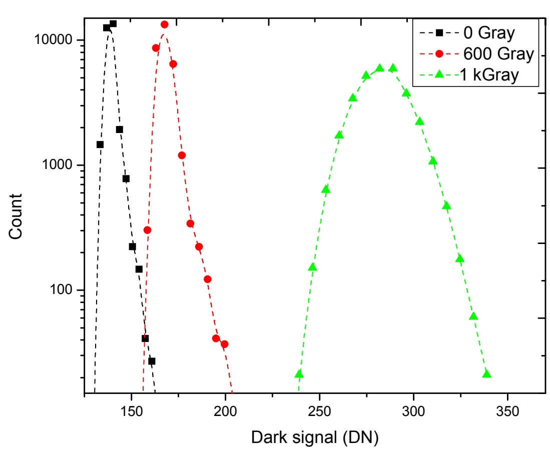

Figure 4: Histogram of the dark signal for sensor with NTA=0.2 µm, p-well protected.

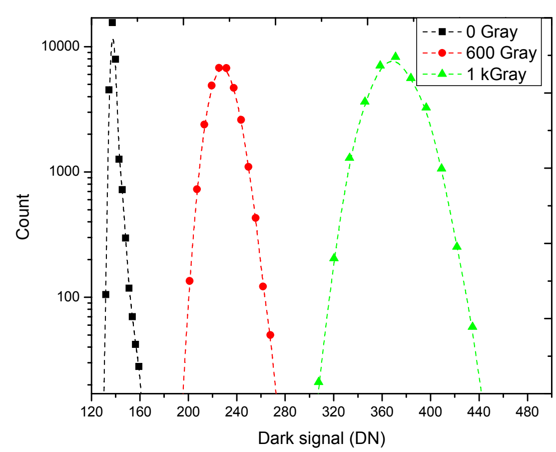

Figure 5: Histogram of the dark signal for sensor with NTA=0.3 µm, no p-well protection.

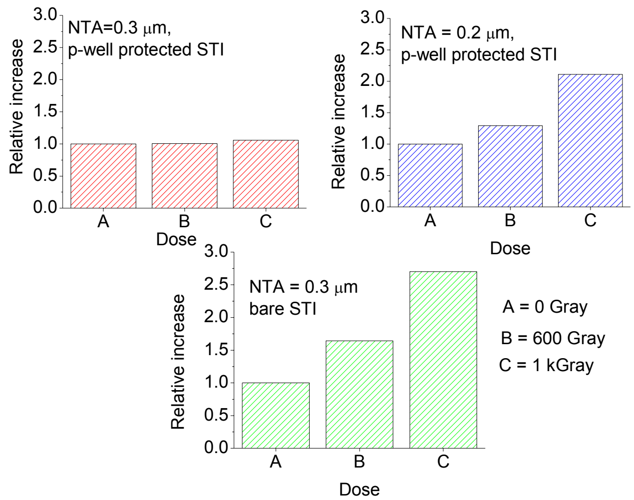

Figure 6: Relative increase in the mean dark signal of the sensors.

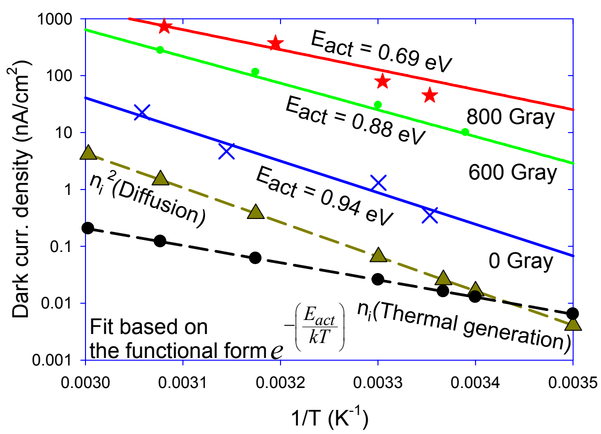

Figure 7: Arrhenius plot of the dark current of sensor (NTA=0.3 μm, no p-well).

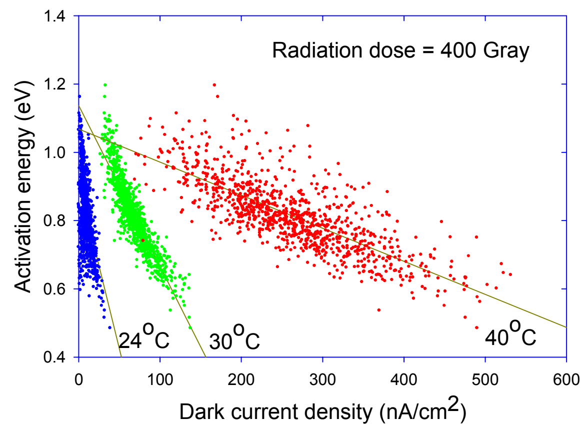

Figure 8: Leakage current vs. activation energy of 1000 pixels (NTA=0.3 μm, no p-well).

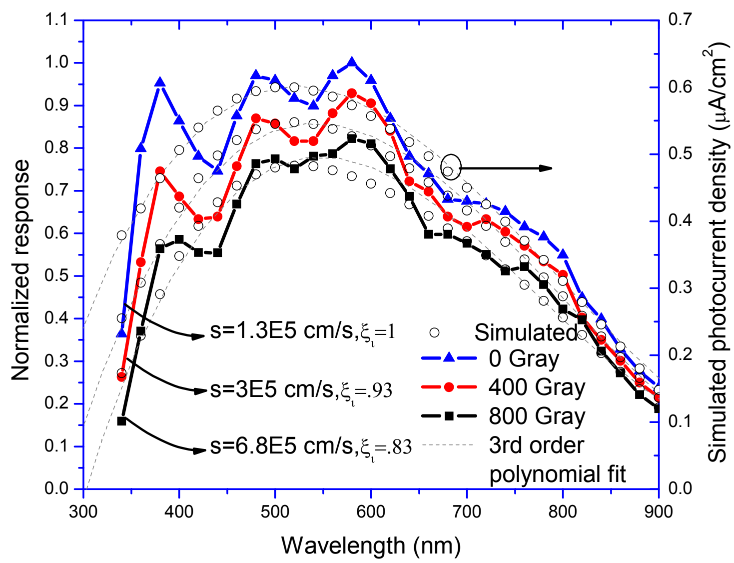

Figure 9: Normalized spectral response of radiated and unradiated sensors (NTA=0.3 μm, no p-well) as a function of wavelength and the fit.